THE JOURNAL OF BIOLOGICAL CHEMISTRY
Vol. 276, No. 40, Issue of October 5, pp. 36961–36969, 2001

Printed in U.S.A.

Identification and Characterization of Novel Mammalian Neuropeptide FF-like Peptides That Attenuate Morphine-induced Antinociception*

Received for publication, June 8, 2001, and in revised form, July 26, 2001
Published, JBC Papers in Press, July 31, 2001, DOI 10.1074/jbc.M105308200

Qingyun Liu‡§, Xiao-Ming Guan¶, William J. Martin‖, Terrence P. McDonald‡, Michelle K. Clements‡, Qingping Jiang‡, Zhizhen Zeng‡, Marlene Jacobson‡, David L. Williams, Jr.‡, Hong Yu¶, Douglas Bomford‖, David Figueroa‡, John Mallee‡, Ruiping Wang‡, Jilly Evans‡, Robert Gould‡, and Christopher P. Austin‡**

From the ‡Department of Pharmacology, Merck Research Laboratories, West Point, Pennsylvania 19486 and the Departments of ¶Metabolic Disorders and ‖Pharmacology, Merck Research Laboratories, Rahway, New Jersey 07065

The two mammalian neuropeptides NPFF and NPAF have been shown to have important roles in nociception, anxiety, learning and memory, and cardiovascular reflex. Two receptors (FF1 and FF2) have been molecularly identified for NPFF and NPAF. We have now characterized a novel gene designated NPVF that encodes two neuropeptides highly similar to NPFF. NPVF mRNA was detected specifically in a region between the dorsomedial and ventromedial hypothalamic nuclei. NPVF-derived peptides displayed higher affinity for FF1 than NPFF-derived peptides, but showed poor agonist activity for FF2. Following intracerebral ventricular administration, a NPVF-derived peptide blocked morphine-induced analgesia more potently than NPFF in both acute and inflammatory models of pain. *In situ* hybridization analysis revealed distinct expression patterns of FF1 and FF2 in the rat central nervous system. FF1 was broadly distributed, with the highest levels found in specific regions of the limbic system and the brainstem where NPVF-producing neurons were shown to project. FF2, in contrast, was mostly expressed in the spinal cord and some regions of the thalamus. These results indicate that the endogenous ligands for FF1 and FF2 are NPVF- and NPFF-derived peptides, respectively, and suggest that the NPVF/FF1 system may be an important part of endogenous anti-opioid mechanism.

The Phe-Met-Arg-Phe-NH_2 (FMRFamide)[1]-related peptides (FaRPs) constitute a large family of neuropeptides that are widely distributed in invertebrates, and function as neurotransmitters and neuromodulators (1, 2). Existence of FaRPs in vertebrates was initially demonstrated by the observation of specific immunoreactive staining in rat brain using anti-FMRFamide antisera (3). The first vertebrate FaRP, Leu-Pro-Leu-Arg-Phe-NH_2 (LPLRFa), was isolated from chicken brain using anti-FMRFamide antisera (4). Two mammalian FaRP-like peptides, NPAF and NPFF, were then isolated from bovine brain by a similar approach (5). Isolation of the gene encoding NPAF and NPFF revealed that the two peptides are generated from the processing of a single large precursor (6, 7).

A great deal of evidence suggests that NPAF and NPFF play important roles in the control of pain and analgesia through interactions with the opioid system (see Refs. 8 and 9 for review). Intracerebroventricular administration of FMRFamide, NPFF, or NPAF attenuated morphine-induced analgesia whereas injection of antisera against FMRFamide or NPFF had the opposite effect (5, 10). Administration of NPFF into morphine-tolerant rats induced symptoms of the withdrawal whereas administration of anti-NPFF IgG reversed morphine tolerance (11, 12). Such observations led to the classification of NPFF as one type of anti-opioid peptides, which have been hypothesized to be partially responsible for the rapid development of opioid tolerance and dependence in animal models and clinical use of opioids (13). NPFF, on the other hand, was also shown to have pro-opioid effect following intrathecal administration (14). Furthermore, recent data indicate that ICV-administrated NPFF was able to attenuate neuropathic pain independent of the opioid system (15). In addition, FMRFamide and NPFF were also shown to affect the cardiovascular system and cause other behavioral changes in mammals (8). Recently, molecular identification of two receptors (FF1 and FF2) have been reported for NPFF and NPAF (16–18). A novel mammalian gene encoding NPFF-like peptides (RFRP1 and RFRP3) and their receptor (OT7T022) was also reported (19). A quail gene encoding neuropeptides highly similar to the chicken peptide LPLRFa was just published (20). Herein we describe the comparison of the two NPFF receptors in their responses to various NPFF-like peptides and in their expression pattern in the rat central nervous system (CNS). We also describe the independent identification of novel NPFF-related peptides (designated NPVF) and their role in attenuating morphine-induced analgesia. Potential roles of the two receptors/four peptide ligands in nociception modulation are discussed.

EXPERIMENTAL PROCEDURES

Molecular Cloning of FF1 and FF2—The full-length coding sequence of human FF2 was isolated and determined by extending the 5′ end of the EST sequence AA449919 (GenBank® accession number) using a strategy described previously (21), and subcloned into the vectors

* The costs of publication of this article were defrayed in part by the payment of page charges. This article must therefore be hereby marked "*advertisement*" in accordance with 18 U.S.C. Section 1734 solely to indicate this fact.

The nucleotide sequence(s) reported in this paper has been submitted to the GenBank™/EBI Data Bank with accession number(s) AF330057–AF330059.

§ To whom correspondence should be addressed. Tel.: 215-652-6592; Fax: 215-652-2075; E-mail: jim_liu@merck.com.

** Current address: Viral Vaccine Technology Development Center, Wyeth Lederle Vaccines, Pearl River, NY 10965.

[1] The abbreviations used are: FMRFamide, Phe-Met-Arg-Phe-NH_2; FaRP, Phe-Met-Arg-Phe-NH_2-related peptide; LPLRFa, Leu-Pro-Leu-Arg-Phe-NH_2; ICV, intracerebral ventricular; CNS, central nervous system; CHO, Chinese hamster ovary; NFAT, nuclear factor of activated T cells; EST, expressed sequence tag; FLIPR, fluorescence imaging plate reader.

pcDNA3.1(−) (Invitrogen, Inc.) and pIRESpuromycin (CLONTECH, Inc.). Full-length coding sequences of human and rat FF1 were amplified by polymerase chain reaction and cloned into expression vectors as above based on the published sequences of the receptor B5 (41).

Functional and Binding Assays—CHO-NFAT-bla and HEK293-CRE-bla cells (22) were obtained from Aurora Biosciences. They were transfected with human FF1/pIRESpuromycin or FF2/pIRESpuromycin with CHO-NFAT-bla cells co-transfected with a plasmid containing the chimeric G protein $G\alpha_{qi5}$ (23). Stable cell lines from CHO-NFAT-bla cells showing strong agonist response were generated by fluorescence-activated cell sorting as described (22). Fluorescence imaging plate reader (FLIPR) and β-lactamase assays were performed as described (22, 24). Inhibition of forskolin-stimulated cAMP was carried out with HE293-CRE-bla cells stably expressing FF1 or FF2 following treatment of 10 μM forskolin for 10 min using the scintillation proximity assay kit (Amersham Pharmacia Biotech). Radioligand binding analyses were performed on cellular membranes prepared from CHO-NFAT-bla cells stably expressing human FF1 or FF2 and $G\alpha_{qi5}$ as described previously (25). [Tyr^{30}]hNPSF-(30–37) (Y-A-N-L-P-L-R-F-NH_2) and [Tyr^1]NPFF (Y-L-F-Q-P-Q-R-F-NH_2) were labeled with ^{125}I at its N-terminal tyrosine residue (Woods Assay, Portland, OR) to a specific activity of ~2,000 Ci/mmol. All peptides were purchased from Phoenix Pharmaceuticals, Inc.

Identification and Cloning of NPVF—The entire EST data base (GenBank™ dbEST) was searched with query sequences LPLRFGR and LPLRFGK. One EST (GenBank™ accession no. R84948) appeared to encode LPLRFGR and was extended to a full-length open reading frame by searching for additional EST and genomic sequences. Partial sequences of the mouse and rat orthologs of this human gene were isolated by degenerate polymerase chain reaction on genomic DNA template using degenerate primers for LPLRFGR (forward) and LPQRFGR (reverse). Species-specific primers were then synthesized and used to clone and sequence flanking genomic fragments with the GenomeWalker kit (CLONTECH, Inc.). Comparison of the mouse and rat genomic sequences with human genomic and cDNA sequences identified the exon-intron boundaries as well as the open reading frames of the two rodent genes.

In Situ Hybridization and Immunohistochemistry Analysis—For rat brain analysis, male Sprague-Dawley (Charles River) rats were killed by decapitation under CO_2, and brains were quickly removed and frozen in −40 °C isopentane. Fourteen-μm coronal sections were cut on a cryostat and hybridized with ^{33}P-labeled oligonucleotide probes as described previously (26). The sequences of the antisense oligonucleotide probes are 5′-CTGCTGAGTGGGGCACTTTGTTGGCAGGGGCTGGACTCATCTTAA-3′ or 5′-TCTGGCTGTTGTTCTCCCAAACCTTTGGGGCAGGTTG-3′ for NPVF; an equal molar mixture of 5′-GTAGGAGGAGAAGGTGAGGCTGGTTGCTATGCTGGTCTCCACATC-3′, 5′-CACCAGTGTGAAAACCGATGCAGACACGGACATGCCCTGCACCAA-3′, and 5′- GTTACGAGCATCCAGCATGAAGTGATGCTCCTCTCGGGTGACTGT-3′ for FF1, and 5′- TTGATATCTGAATACCAAGGATGCTGTGTGTCATTGCCACTCCAG-3′, 5′-ACCATGCACAGGAAGAAGATCAGGAAGTAGGAGCTAATGAAGACAG-3′, and 5′- CCGTGTGCATGTACCTATTCCTTATTACAACAAAGCAAACGACAGT-3′ for FF2.

Behavioral Experiments—ICV cannulae were placed in the left lateral ventricle of male Harlan Sprague-Dawley rats (250–350 g; Charles River). Rats were housed in pairs on a 12-h light/dark cycle, were given free access to food and water, and were handled by an investigator for at least 3 days prior to testing. Test substances were dissolved in sterile saline and were administered in a volume of 5.0 μl. For the hot plate assay, rats were placed on a 52.5 °C hot plate and the latency to hindpaw licking was measured. Hot plate latencies were determined before (three times) and 5, 15, 30, and 60 min after ICV injection. We used a 30-s cut-off latency to avoid skin damage. For the formalin test, vehicle or test substance was administered 60 min after animals were acclimated to a Plexiglas cylinder (15 cm diameter) and 5 min before a 50-μl injection of formalin (5%) into dorsal hindpaw. The number of flinches were counted continuously for 60 min using an automated nociception analyzer (UCSD Anesthesiology Research, San Diego, CA). The mean of three pre-treatment hot plate latencies were used to compare the effect of treatment. The maximum possible effects were determined. Area under the curve was calculated during the 60 min after administration. Statistical significance for treatment groups in both hot plate and formalin tests was determined by one-way analysis of variance followed by Dunnett's multiple comparisons *post hoc* test (Prism, GraphPad Inc., San Diego, CA).

All rodent experiments were reviewed and approved by the Institutional Care and Animal Use Committee at Merck Research Laboratories (Rahway, NJ) and conform to the guidelines on the study of pain in awake animals established by the International Association for the Study of Pain (27).

RESULTS

Differential Activation of FF1 and FF2 by FaRPs—In searching for novel G protein-coupled receptors, we identified a human EST sequence (GenBank™ accession no. AA449919) and cloned its full-length coding sequence, which was initially designated HG31 (data not shown). We then screened for agonists of HG31 and found that NPFF and NPAF could bind and activate HG31 with high affinity (data not shown). The amino acid sequence of HG31 is identical to the recently described human NPFF receptor FF2 and HLWAR77 (16, 17), and herein the designation FF2 is adopted. Searching of a sequence database of patent applications with FF2 identified another orphan G protein-coupled receptor named B5 (41), which has an overall homology of ~50% with FF2 at the amino acid level (data not shown). We cloned the B5 receptor and found that it also responded to NPFF and NPAF with high affinity (data not shown). Sequence comparison revealed that B5 is identical to the recently described NPFF receptor FF1 (17) and the RFRP receptor OT7T022 (19). The term FF1 is herein used to described B5/OT7T022.

We determined that both FF1 and FF2 were activated by NPFF and NPAF with high affinity through coupling to the $G\alpha_{i/o}$ pathway (data not shown), consistent with recent publications (16, 17, 19). To carry out further analysis of the two receptors, cell lines stably expressing FF1 or FF2 and the chimeric G protein $G\alpha_{qi5}$ were generated from the cell line CHO-NFAT-bla, which harbors the reporter enzyme β-lactamase under the control of the Ca^{2+}-sensitive enhancer NFAT (22, 23, 28). Cells expressing FF1 showed a robust, dose-dependent increase in β-lactamase activity in response to human NPFF (EC_{50} = 10 nM, Fig. 1*A*), and to the chicken peptide LPLRFa with, surprisingly, a higher affinity (EC_{50} = 3.3 nM, Fig. 1*A*). In contrast, cells expressing FF2 showed high affinity response to NPFF (EC_{50} = 3.3 nM, Fig. 1) but poor affinity for LPLRFa (EC_{50} > 1,000 nM, Fig. 1*B*). The responses were also examined by the FLIPR assay, which measures Ca^{2+} mobilization directly. Again, cells expressing FF1 showed higher affinity for LPLRFa (Fig. 1*C*, EC_{50} = 2.4 nM) than for human NPFF (Fig. 1*C*, EC_{50} = 15 nM) with the approximately the same level of maximum response to both peptides (Fig. 1*C*). In contrast, cells expressing FF2 showed strong, high affinity response only to human NPFF (Fig. 1*D*, EC_{50} = 2 nM). Since LPLRFa was only isolated from chicken brain at the time of these experiments, the data suggested the existence of a mammalian ligand more similar to LPLRFa for FF1 and prompted us to search for such peptides.

Identification of Mammalian LPLRFa-like Peptides—To find potential mammalian LPLRFa-encoding genes, the GenBank™ EST data base was searched using query sequences LPLRFGR and LPLRFGK (GR and GK were added on since they are obligatory sequences required for cleavage and amidation) using the program tblastn (29). One human EST (GenBank™ accession no. R84948) was found to encode such potential peptides. Assembly and analysis of additional EST and genomic sequences in GenBank™ resulted in a complete open reading frame of 543 base pairs encoding a peptide of 180 amino acids (Fig. 2*A*). The predicted polypeptide appears to contain two potential mature peptides terminating with similar structures at the C terminus. Based on the rules of neuropeptide processing (30, 31), the first peptide was predicted to be a 37-amino acid peptide consisting of amino acid residues 56–92 (Ser-37-Phe-amide) and was designated NPSF-(1–37); the second peptide was predicted to contain eight amino acids corresponding

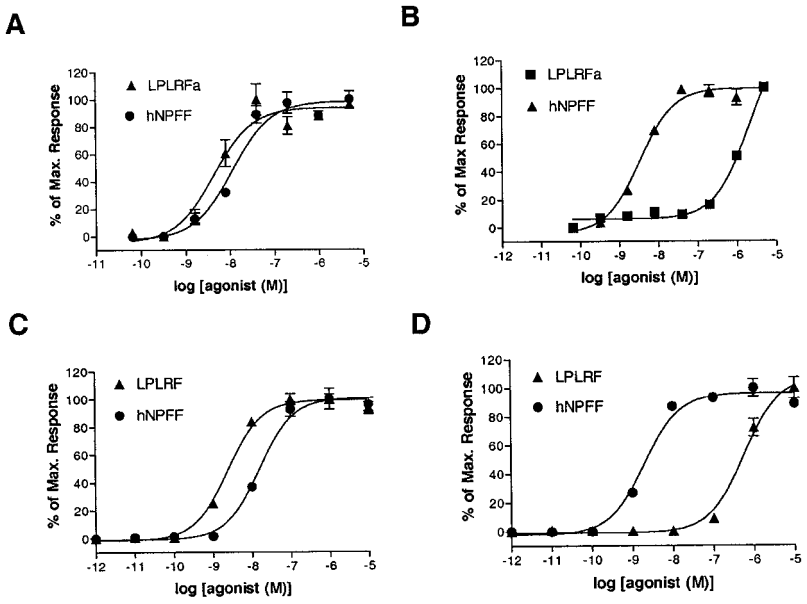

FIG. 1. **Activation of FF1 and FF2 by human NPFF and chicken LPLRFa.** *A* and *B*, dose-dependent responses of FF1 (*A*) and FF2 (*B*) stably expressed in CHO-NFAT-bla cells co-expressing $G\alpha_{qi5}$ in the β-lactamase assay. *C* and *D*, dose-dependent responses of FF1 (*C*) and FF2 (*D*) of the same cell lines in the FLIPR assay. All results shown are the means ± S.E. of triplicate determinations.

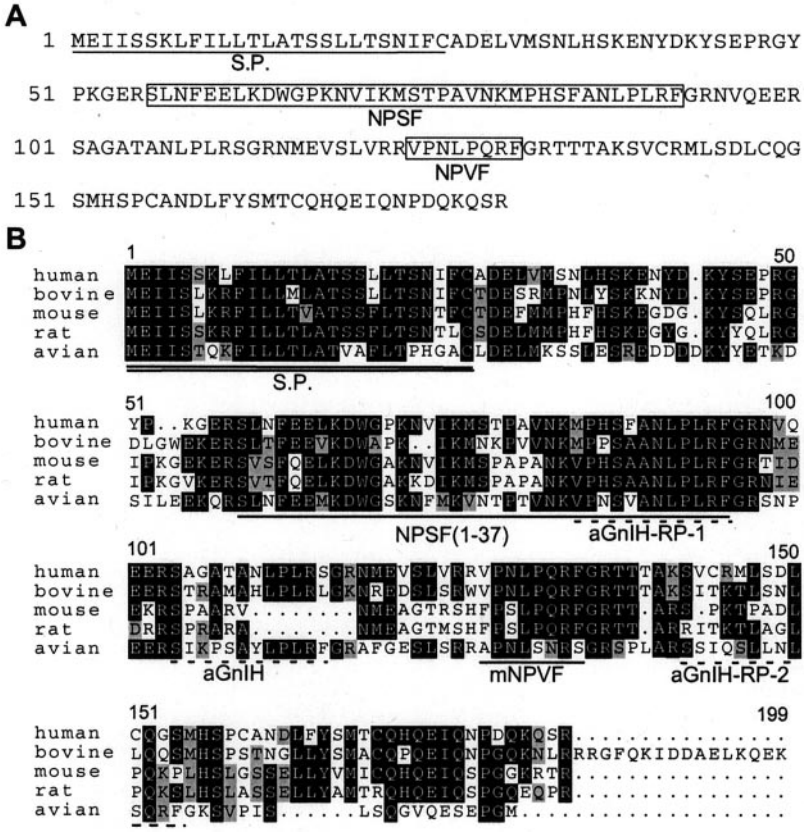

FIG. 2. **Sequence of human NPVF precursor and its alignment with species orthologs.** *A*, predicted polypeptide sequence of human NPVF. The signal peptide sequence (*S.P.*) is *underlined*. The two potential mature peptides, NPSF-(1–37) and NPVF, are *boxed*. *B*, alignment of the polypeptide sequences of the NPVF precursors of human, bovine, mouse, rat, and quail. The predicted signal peptide sequence (*S.P.*), NPSF, and NPVF are *underlined*. The peptides predicted only in the quail precursor are *underlined* with *dashed line*. The GenBank™ accession numbers are as follows: human NPVF, AF330057; mouse NPVF, AF330058; rat NPVF, AF330059; bovine NPVF, AB040291; chicken GnIH, AB039815.

to amino acid residues 124–131 (Val-8-Phe-amide) and was designated NPVF (Fig. 2*A*). The gene was designated NPVF to distinguish it from the NPFF gene. The mouse and rat orthologs of NPVF were also isolated and found to be highly homologous to human one around the predicted peptides (Fig. 2*B*). While this work was in progress, Hinuma *et al*. described a gene (called RFRP) encoding two potential neuropeptides (RFRP-1 and RFRP-3), which turned out to be same gene as NPVF (19). Just recently, an avian gene encoding three potential FaRPs was isolated from the quail (20). Alignment of the polypeptide sequences from these five species, human, mouse, rat, bovine, and quail, revealed that they are highly conserved around the predicted signal peptide and mature neuropeptide sequences, indicating that they are most likely to be species orthologs (Fig. 2*B*).

For all these precursors, it is relatively straight forward to predict their C-terminal cleavage and processing sites of mature peptides since they must be Arg-Phe-Gly followed by a monobasic or double basic motif. The N-terminal cleavage sites, however, are not always obvious. For the quail gene, two peptides, GnIH and GnIH-RP-2 of the predicted peptides, were actually identified from brain extracts (20). Neither of the two peptides, however, are conserved in the mammalian orthologs (Fig. 2*B*). On the other hand, the quail gene appeared to have lost the mammalian peptide NPVF (Fig. 2*B*). For the isolated quail peptides, N-terminal cleavage used the first Arg-Ser se-

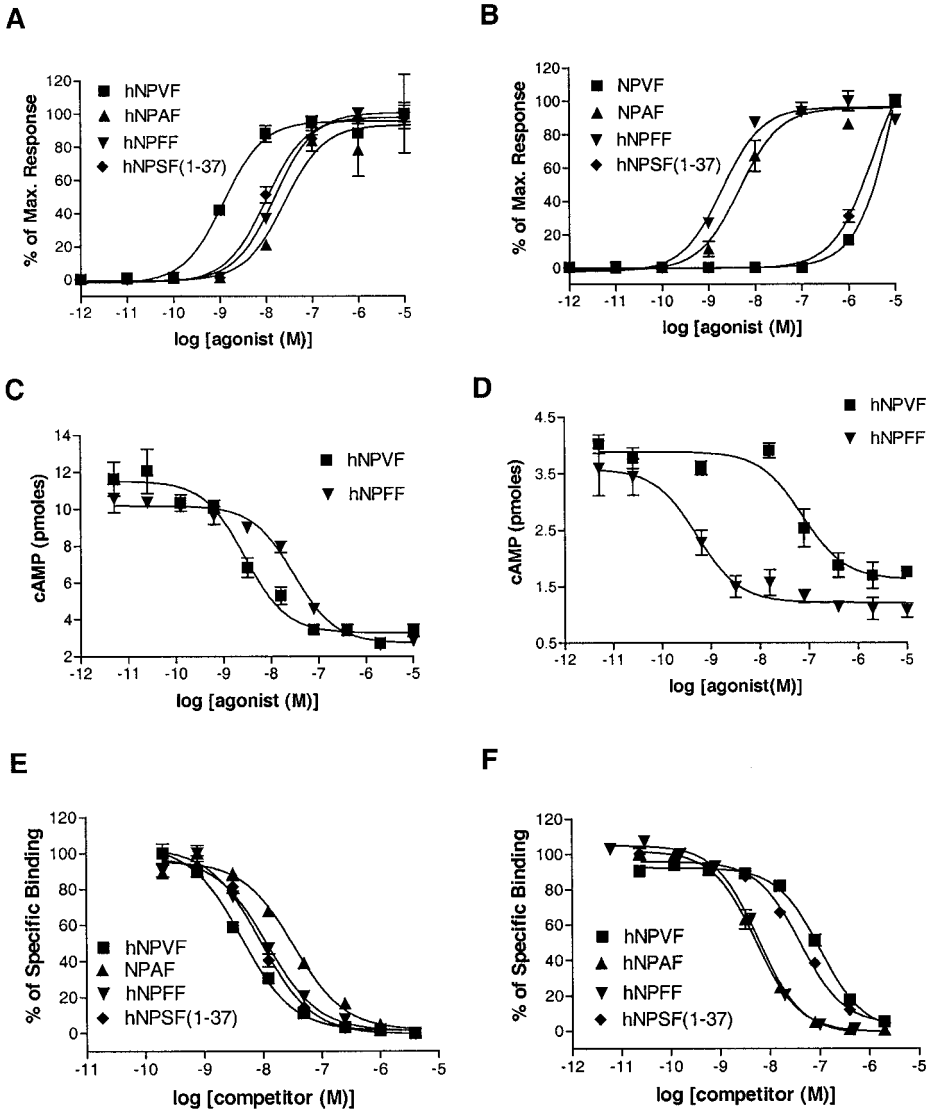

FIG. 3. **Activation of FF1 and FF2 by NPFF- and NPVF-related peptides.** *A* and *B*, dose-dependent activation of FF1 (*A*) and FF2 (*B*) stably expressed in CHO-NFAT-bla cells co-expressing $G\alpha_{qi5}$ in the FLIPR assay. *C* and *D*, dose-dependent inhibition of forskolin-stimulated cAMP in HEK293-CRE-bla cells stably expressing human FF1 (*C*) or FF2 (*D*). *E* and *F*, radioligand competition binding analysis of FF1 (*E*) and FF2 (*F*) using cellular membranes prepared from the same cell lines. All results shown are the means ± S.E. of triplicate determinations.

quence motif upstream of the C-terminal cleavage site (Fig. 2*B*). For the identity of NPSF, Hinuma *et al*. (19) and Satake *et al*. (20) predicted the N-terminal cleavage occurred at the first lysine residue upstream of the C-terminal cleavage site, which would give a mature peptide containing 12 amino acids following by amidation. However, such a predicted quail peptide GnIH-RP-1 could not be identified from the brain extracts along with GnIH and GnIH-RP-2 (20). Interestingly, the region upstream of the GnIH-RP-1 is also highly conserved (Fig. 2*B*). One Arg-Ser motif, conserved across the five species, was found 36 amino acid residues upstream of the predicted C-terminal cleavage site (Fig. 2*B*). Thus, this motif is most likely to provide the N-terminal cleavage site of NPSF despite three lysine residue in between for the following reasons: Arg-Ser was used for the other two peptides of the same precursor in the quail, the sequence between this motif and the Arg-Phe motif are highly conserved, and mono-lysine sites in general are much less efficient than mono-arginine sites (30, 31). The true identity of these peptides can only be determined by structural analysis of purified peptides.

Activation and Binding of FF1 and FF2 by NPFF and NPVF Peptides—A series of peptides predicted from the human and rat NPVF precursors were then synthesized and examined on FF1 and FF2. In the FLIPR assay, the octapeptide human NPVF showed better affinity than NPFF for FF1 (1.2 nM *versus* 15 nM in EC_{50}, Fig. 3*A* and Table I). The human NPSF-(1–37) displayed approximately the same affinity as NPFF did for FF1 (Fig. 3*A*). In contrast, both human NPVF and NPSF-(1–37) showed poor agonist affinity for FF2 (EC_{50} > 1,000 nM for both peptides) while NPFF and NPAF showed potent activity (Fig. 3*B* and Table I). The responses of FF1 and FF2 to NPVF peptides were also examined by measuring inhibition of forskolin-stimulated cAMP production. HEK293 cells stably expressing human FF1 or FF2 showed strong inhibition of forskolin-stimulated cAMP in response to both NPVF and NPFF. Again, FF1 showed higher affinity to NPVF (EC_{50} = 2.9 nM) than to NPFF (EC_{50} = 31 nM) (Fig. 3*C*), whereas FF2 showed much better affinity to NPFF (EC_{50} = 0.6 nM) than to NPVF (EC_{50} = 74 nM) (Fig. 3*D*).

Radioligand binding analysis were then carried out on both FF1 and FF2. Saturation binding analysis showed specific, saturable, and high affinity binding of NPFF to FF1 and NPVF to FF2 (data not shown), consistent with the published results (16, 17, 19). Competition binding analyses were then performed to compare the affinities of various peptides. Using ^{125}I-labeled Tyr^{30}-NPSF-(30–37), both NPVF and NPSF-(1–37) displayed high affinity, complete displacement of the radioligand whereas NPFF showed significant lower affinity (Fig. 3*E* and Table I). On the other hand, NPFF and NPAF showed much better affinity for FF2 than human NPVF and NPSF-(1–37)

TABLE I

Functional and binding affinities of various peptides on human FF1 and FF2 stably expressed in CHO-NFA-bla cells coexpressing the chimeric G protein $G\alpha_{qi5}$

Functional affinities (EC_{50}, nM) were determined by the FLIPR assay; binding affinities (IC_{50}, nM) were determined by radioligand competition binding assay using ^{125}I-labeled 1-Tyr-hNPSF-(30–37) for FF1 and ^{125}I-labeled 1-Tyr-NPFF for FF2.

Name	Sequence	FF1		FF2	
		EC_{50} (SD)	IC_{50} (SD)	EC_{50} (SD)	IC_{50} (SD)
hNPSF-(1–37)	SLNFEELKDWGPKNVIKMSTPAVNKMPHSFANLPLRF-NH2	12.0 (2.0)	9.1 (1.3)	560 (60)	7.5 (0.8)
rNPSF-(1–37)	SVTFQELKDWGAKKDIKMSPAPANKVPHSAANLPLRF-NH2	10.1 (1.1)	10.3 (3.3)	3,398 (247)	13.2 (1.5)
rNPSF-(15–37)	DIKMSPAPANKVPHSAANLPLRF-NH2	6.1 (0.6)	6.4 (1.4)	8,071 (633)	58.2 (7.3)
hNPSF-(26–37)	MPHSPANLPLRF-NH2	11.0 (1.3)	3.1 (0.6)	242 (21)	6.1 (0.5)
hNPVF	VPNLPQRF-NH2	1.2 (0.1)	4.4 (0.5)	1,244 (138)	122.3 (17.8)
Y^{30}-hNPSF-(30–37)	YANLPLRF-NH2	ND[a]	1.4 (0.2)	ND	12.5 (1.2)
LPLRFa	LPLRF-NH2	2.4 (0.3)	8.1 (2.1)	568 (70)	7.3 (0.8)
hNPAF	AGEGLSSPFWSLAAPQRF-NH2	24.9 (10.1)	33.4 (9.3)	4.7 (0.8)	3.3 (0.4)
hNPFF	SQAFLFQPQRF-NH2	15.6 (1.6)	11.8 (3.3)	2.0 (0.2)	1.1 (0.1)
bNPFF	FLFQPQRF-NH2	14.3 (1.7)	6.2 (1.2)	19.3 (1.5)	3.1 (0.3)
Y1-bNPFF	YLFQPQRF-NH2	ND	13.5 (1.5)	ND	3.0 (0.3)
(1DNMe) bNPFF	(d)YL(Nme)FQPQRF-NH2	13.8 (1.8)	5.6 (1.0)	11.6 (1.0)	3.4 (0.4)
FMRFamide	FMRF-NH2	22.9 (2.7)	3.1 (0.1)	680 (31)	7.8 (1.5)

[a] ND, not determined.

(Fig. 3*F* and Table I). The functional and binding data indicated that NPVF-derived peptides were more potent ligands for FF1 whereas NPFF-derived peptides were the only high affinity ligands for FF2.

In Situ Hybridization Analysis of NPVF—To determine the expression pattern of NPVF, *in situ* hybridization analysis was carried out in the rat brain using two non-overlapping oligonucleotide probes. The two probes gave virtually identical expression patterns, which are represented in Fig. 4*A*. Specific expression of NPVF was only detected in the region between the dorsomedial hypothalamic and ventromedial hypothalamic nucleus, consistent with the data from Hinuma *et al.* (19). No expression of NPVF was detected in any other region of the rat CNS (data not shown). This specific pattern of expression, interestingly, matched an immunohistochemical staining pattern previously observed with anti-NPFF antisera in the rat hypothalamus (7, 32). Furthermore, this region had no expression of the NPFF gene, which originally led to the hypothesis that other distinct NPFF-like peptides were produced by these neurons (7). Given the strong structure similarity between NPFF and NPVF, and the robust specific expression of NPVF in this region, it is highly likely that NPVF-encoded peptides correspond to the immunoreactivity previously detected there with anti-NPFF antisera.

Expression of FF1 and FF2 in Rat CNS—The CNS distribution of FF1 and FF2 expression was examined by *in situ* hybridization analysis throughout the entire rat CNS. The two receptors exhibited strikingly distinct pattern of expression (Table II). FF1 was much more broadly distributed. The strongest signals were detected in the lateral septum, especially the intermediate and dorsal part of the lateral septal nuclei, and in various thalamic nuclei including the parafascicular, anterodorsal, reticular, and anterior paraventricular thalamic nuclei (Fig. 5 (*A* and *B*) and Table II). Hypothalamus was another major site of expression for FF1 (Fig. 5, *C* and *D*). Moderate to strong signals were observed in the paraventricular, medial preoptic, anterior, dorsomedial, and ventromedial hypothalamic nuclei. In addition, significant expression of FF1 was detected in the amygdala, primarily in the central, medial, and basolateral amygdaloid nuclei (Fig. 5*D*). Finally, low to moderate hybridization was also detected in a number of other brain regions such as the bed nucleus of the stria terminalis, periaqueductal gray, dorsal raphe, pars compacta of the substantia nigra, locus coeruleus, lateral parabrachial nucleus, area postrema, and dorsal motor nucleus of the vagus (Table II). Interestingly, no expression of FF1 was detected in the

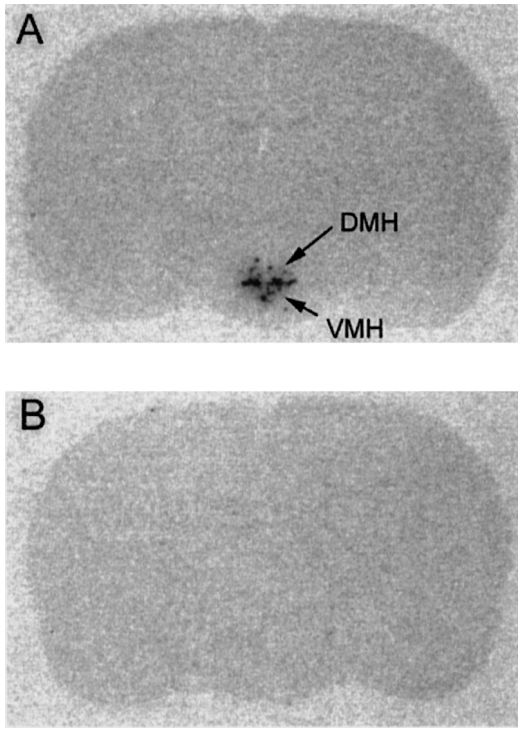

FIG. 4. ***In situ* hybridization analysis of NPVF in rat brain in the absence (*A*) or presence (*B*) of 100-fold excess of unlabeled probes using ^{33}P-labeled antisense oligonucleotide.** *DMH*, dorsomedial hypothalamic nucleus; *VMH*, ventromedial hypothalamic nucleus.

spinal cord. In contrast, FF2 expression was much more limited (Table II). Modest to high levels of FF2 were found in the centrolateral and parafascicular nuclei of the thalamus (Fig. 6, *A–C*). Low to moderate signals were also detected in the reticular, dorsomedial part of laterodorsal, and centrolateral nuclei of the thalamus, and in the lateral hypothalamic area, anterior pretectal nucleus, medial and supramammillary nuclei, ventral pontine reticular nucleus, lateral parabrachial nucleus, nucleus of the solitary tract, and dorsal motor nucleus of the vagus (Fig. 6 (*A–C*) and Table II). Strong expression of FF2 was noted in the superficial laminae (I/II) of the dorsal horn and near the central canal (laminae X) of the spinal cord at all levels examined (*i.e.* thoracic, lumbar, and sacral regions) (Fig. 6*E*). Specific hybridization signals were not observed in the

TABLE II
Distribution and relative abundance of FF1 and FF2 mRNA in the rat CNS

The relative densities were estimated using a four-point scale: +++, highest density; ++, moderate density; +, low, but above the background; −, indistinguishable from the background intensity.

	FF1	FF2
Piriform cortex	+	−
Nu accumbens	+	−
Intermediate part of lateral septal nu	+++	−
Dorsal part of lateral septal nu	+++	−
Ventral part of lateral septal nu	++	−
Bed nu of stria terminalis	++	−
Lat part of interstitial nu of post. limb of ant. commissure	+	−
Subfornical organ	+	−
Reticular thalamic nu	++	++
Dorsomedial part of the laterodorsal thalamic nu	−	++
Anterodorsal thalamic nu	+++	−
Anterior paraventricular thalamic nu	++	−
Centrolateral thalamic nu	−	++
Parafascicular thalamic nu	+++	+++
Central medial thalamic nu	+	−
Paracentral thalamic nu	+	−
Reuniens thalamic nu	+	−
Paraventricular thalamic nu	+	−
Anterior pretectal nu	−	+
Olivary pretectal nu	+	−
Medial pretectal nu	+	−
Posterior pretectal nu	+	−
Retrochiasmatic area	+	−
Medial preoptic nu	++	−
Anteroventral periventricular nu	+	−
Suprachiasmatic nu	+	−
Anterior hypothalamic	++	−
Paraventricular hypothalamic nu	+++	−
Lateral hypothalamic area	−	++
Ventromedial hypothalamic nu	++	−
Dorsomedial hypothalamic nu	++	−
Dorsal tuberomammillary nu	++	−
Medial mammillary nu	+	+
Supramammillary nu	−	+
Tuberomammillary nu	+	−
Zona incerta	+	−
Central amygdaloid nu	++	−
Medial amygdaloid nu	++	−
Basomedial amygdaloid nu	+	−
Anterior cortical amygdaloid nu	+	−
Basolateral amygdaloid nu	++	−
Medial and lateral habenular nu	+	−
Pars compacta of the substantia nigra	+	−
Superior colliculus	+	−
Nu of the brachium of the inferior colliculus	+	−
External cortex of the inferior colliculus	+	−
Medial geniculate nu	+	−
Dorsolateral periaqueductal gray	+	−
Lateral periaqueductal gray	+	−
Oculomotor nu	+	−
Dorsal raphe nu	+	−
Median raphe nu	+	−
Caudal linear nu of raphe	+	−
Interpeduncular nu	+	−
Dorsal tegmental nu	−	+
Laterodorsal tegmental nu	+	−
Locus coeruleus	+	−
Lateral parabrachial nu	+	+
Ventral pontine reticular nu	−	++
Area postrema	++	−
Nu of the solitary tract	−	++
Dorsal motor nu of the vagus	+	+
Spinal cord		
lamina I/II	−	++
lamina X	−	+

hippocampus, cerebellum, and cerebral cortex for either receptor.

Anti-opioid Effects of NPVF—Since NPFF activates both FF1 and FF2 with high affinity, it is not clear which receptor (FF1, FF2, or both) mediates the anti-opioid effects of NPFF observed previously (5). Given its structure similarity with NPFF and its preferential activation of FF1, we tested whether NPVF had anti-opioid effect in the hot plate assay and formalin assay. Base-line hot plate latency did not differ among treatment groups (11.2 ± 0.3 s). Morphine (1.3–13.1 nmol/5 μl) dose-dependently increased hot plate latency ($p < 0.0001$), with the highest dose producing near-maximal antinociception (94.1 ± 3.2% MPE (maximal possible effect); Fig. 7*A*). ICV administration of rat NPSF-(1–37) (0.3–10.0 nmol/5μl) did not affect hot plate latencies when given alone (not shown). However, co-administration of rat NPSF-(1–37) (1.0 nmol) and morphine produced a 2.5-fold rightward shift in the morphine dose-response curve and completely blocked the antinociceptive effects of the 2.6-nmol dose of morphine (Fig. 7*A*). In contrast, NPFF by itself decreased hot plate latencies at doses of 1.0 and 3.0 nmol, but at 1.0 nmol only significantly inhibited the antinociceptive effects produced by the 6.6-nmol dose of morphine. Thus, NPVF was more potent than NPFF at blocking morphine-induced antinociception in a model of acute pain. In the formalin model of persistent pain, morphine (2.6 nmol) significantly inhibited the number of flinches during the 60 min after injection (88 ± 3%). Neither NPSF-(1–37) nor NPFF had any effect on formalin-induced nociceptive behavior. However, consistent with the results from the hot-plate test, NPSF-(1–37) (1.0 nmol) caused a 50% reduction in the antinociceptive effects of morphine (44 ± 25%), whereas NPFF (1.0 nmol) led to only a non-significant reduction in morphine's effectiveness (61 ± 10%). The data suggest that the NPVF/FF1 system mediates anti-opioid effects of NPFF.

DISCUSSION

FaRPs constitute a large family of neuropeptides in invertebrates (1, 2). The diversity of FaRPs in vertebrates, however, appears to be more limited. In addition to NPFF, NPAF, and LPLRFa, only one other RFamide neuropeptide, the prolactin-releasing peptide, has been isolated from vertebrates (33). In this report, we described independent identification and characterization of a mammalian gene designated NPVF and its encoded peptides, which most likely represents the mammalian ortholog of the chicken peptide LPLRFa. We also described independent identification and characterization of two NPFF receptors by comparing their affinity for various FaRPs and detailed analysis of their expression pattern in the rat CNS. Furthermore, we showed that NPVF-derived peptides were more potent than NPFF in attenuating morphine-induced analgesia. The molecular pharmacological properties of FF1 and FF2 toward various NPFF and NPVF peptides and their expression pattern in the rat CNS presented here offer new insights into potential mechanisms of the pain-modulatory functions associated with NPFF.

In characterizing affinities of the two receptors to various FaRPs, we noticed FF1 could be activated by many more FaRPs than FF2. Particularly, we were surprised to find that FF1 showed a better response to the chicken peptide LPLRFa than to NPFF, which led to the search for mammalian LPLRFa-like peptides and the eventual identification of NPVF. In the report by Bonini *et al*. (17), FF1 showed much lower affinity to NPFF (EC_{50} = 16 nM) than FF2 did (EC_{50} = 2.0 nM). But no data were presented for LPLRFa. Hinuma *et al*. (19) discovered NPVF by looking for mammalian LPLRFa-like peptides directly and then tested them on the orphan receptor FF1/OT7T022. We have now carried out a side-by-side comparison of NPFF- and NPVF-related peptides on FF1 and FF2, and the *in vitro* data presented here and those from Hinuma *et al*. (19) clearly indicated that NPVF-related peptides are more potent ligands for FF1 and NPFF-related peptides are much better ligands for FF2.

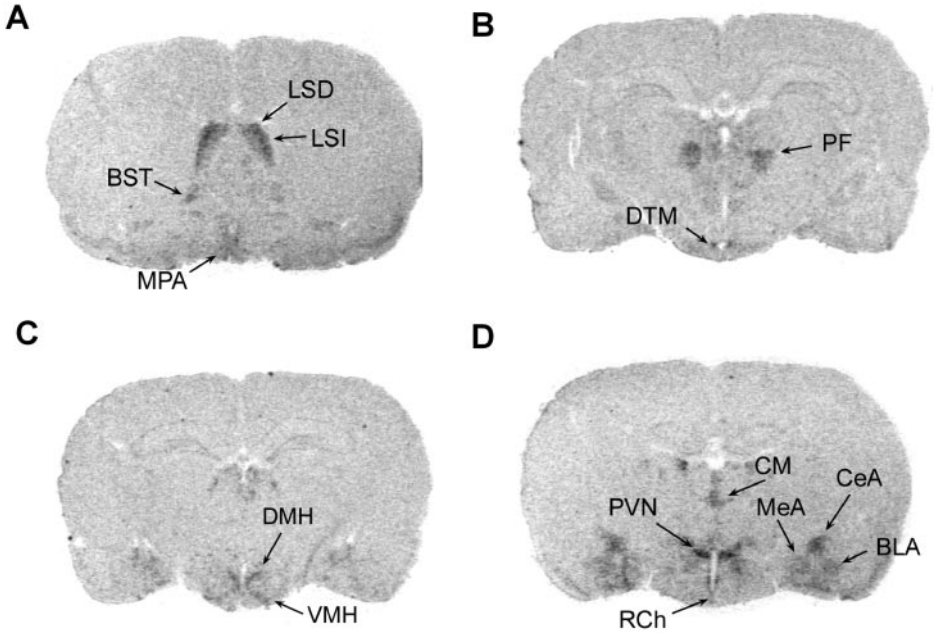

FIG. 5. ***In situ*** **hybridization analysis of FF1 in the rat brain coronal sections using ^{33}P-labeled antisense oligonucleotide probes.** *A*, *BST*, bed nucleus of stria terminalis; *LSD*, lateral dorsal septal nucleus; *LSI*, lateral intermediate septal nucleus; *MPA*, medial preoptic area. *B*, *PF*, parafasicular thalamic nucleus; *DTM*, dorsal tuberomammilary nucleus. *C*, *DMH*, dorsomedial hypothalamic nucleus; *VMH*, ventromedial hypothalamic nucleus. *D*, *BLA*, basolateral amygdaloid nucleus; *CM*, central medial thalamic nucleus; *CeA*, central amygdaloid nucleus; *MeA*, medial amygdaloid nucleus; *PVN*, paraventricular hypothalamic nucleus; *RCh*, retrochiasmatic area. All signals were competed off in the presence of 100-fold excess of unlabeled probes (data not shown).

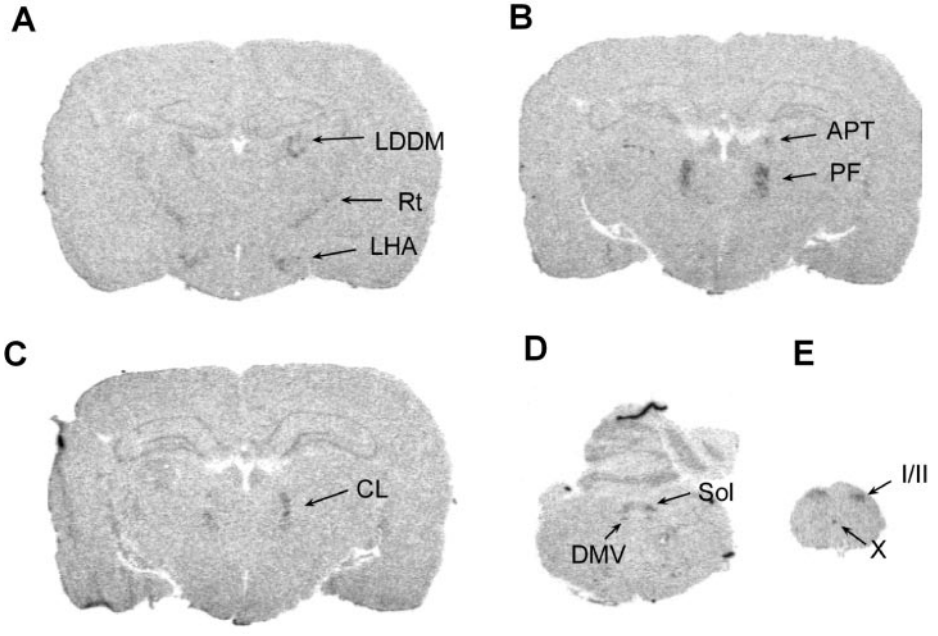

FIG. 6. ***In situ*** **hybridization analysis of FF2 in rat coronal brain sections using ^{33}P-labeled antisense oligonucleotide probes.** *A*, *LDDM*, dorsomedial part of lateral thalamic nucleus; *LHA*, lateral hypothalamic nucleus; *Rt*, reticular thalamic nucleus. *B*, *APT*, anterior pretectal nucleus; *PF*, parafasicular thalamic nucleus. *C*, *CL*, centrolateral thalamic nucleus. *D*, *DMV*, dorsal motor nucleus of vagus; *Sol*, nucleus of the solitary tract. *E*, *I/II*, laminae I and II of the spinal cord; *X*, laminae X. All signals were competed off in the presence of 100-fold excess of unlabeled probes (data not shown).

We mapped the expression pattern of both FF1 and FF2 in the entire rat CNS by *in situ* hybridization, and the data were nearly completely consistent with the results from radioligand binding analysis. Using ^{125}I-labeled (1DNme)bNPFF, which turned out to have equal affinities to rat FF1 and FF2 (17), Dupouy *et al*. (34) mapped NPFF binding sites in the entire rat CNS. Specific binding was detected widely in the CNS with intense signals in the parafascicular, reticular thalamic nuclei, lateral septum, and nucleus of the solitary tract, and in the superficial layers in the dorsal horn and around central canal of the spinal cord, but only a single class of binding was noticed. Examination of FF1 and FF2 expression by *in situ* hybridization has now allowed us to compare the distribution of the two receptors. FF1 is much more widely expressed, with especially strong signals in brain regions regulating the expression of fear and anxiety, and affective aspects of pain (35, 36). FF2 mRNA levels, on the other hand, are much more limited, with the highest levels found in the spinal cord. It is of interest to note, however, that some discrepancies exist between the patterns of receptor binding and receptor mRNA expression. For example, high density NPFF bindings were observed in the presubiculum and spinal trigeminal tract nucleus (34, 37), but these brain regions express little or no detectable FF1/FF2 mRNA. Although the precise reason for such mismatch is unknown, it could be due to subtle differences between the iodinated NPFF analogues used as the radioligands and native NPFF in binding to the receptors or it could be the consequence of transportation of mature/functional receptor proteins (binding sites) away from their origin of synthesis (mRNA), which were measured by autoradiography and *in situ* hybridization, respectively. Alternatively, these results may suggest existence of additional receptor(s) for NPFF.

The genes encoding NPFF and NPVF are similar in structure but distinct in expression pattern, receptor pharmacology,

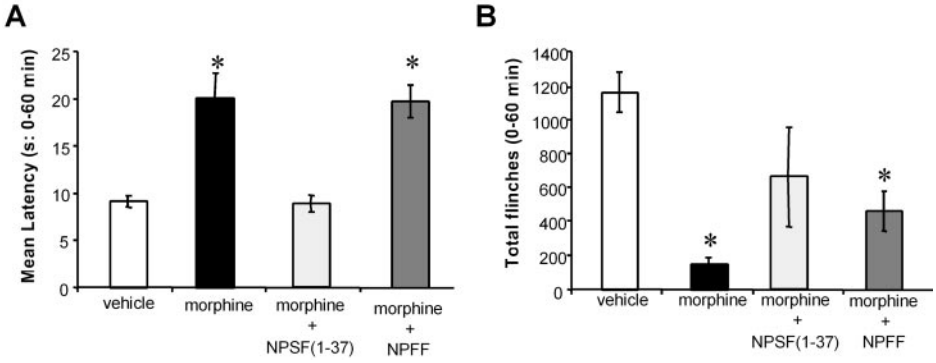

FIG. 7. **Anti-opioid effect of NPFF- and NPVF-related peptides in two models of nociception.** *A*, in the hot plate test, morphine (2.6 nmol/5 μl, ICV) significantly increased the response latency to 52.5 °C thermal stimulus (*, $p < 0.05$). The antinociceptive effects of morphine were blocked when rat NPSF-(1–37) (1.0 nmol) was co-administered ($p > 0.05$ compared with vehicle), whereas co-administration of rat NPFF (1.0 nmol) had no effect on morphine-induced antinociception (*, $p < 0.05$) (vehicle: $n = 37$; treatment: $n = 6–8$/group). *B*, in the formalin model, morphine (2.6 nmol/5 μl, ICV) significantly reduced the total number of flinches produced by formalin injection (5%, 50 μl) into the dorsal hind paw (*, $p < 0.05$). These effects were significantly attenuated when rat NPSF-(1–37) (1.0 nmol) was co-administered ($p > 0.05$ compared with vehicle). However, co-administration of rat NPFF had no effect on morphine-induced antinociception (*, $p < 0.05$) (vehicle: $n = 9$; treatment: $n = 6$/group).

and presumably physiological functions. NPFF is primarily expressed in the paraventricular and supraoptic nuclei of the hypothalamus, the nucleus of the solitary tract, and the superficial layers in the dorsal horn of spinal cord (7), areas with predominant FF2 expression. In contrast, NPVF is only expressed in a population of neurons between the dorsomedial hypothalamic and ventromedial hypothalamic nucleus, which were shown to project to a number of limbic structures including the lateral septal nucleus, bed nucleus of the stria terminalis, amygdala, and hypothalamus as well as to the periaqueductal gray (38), areas where FF1 is strongly expressed. Furthermore, *in vitro* binding and functional analyses also indicate that FF2 can only be activated NPFF-related peptides, whereas FF1 is activated by NPVF-related peptides with a higher affinity than by NPFF-related peptides. Taken together, these data strongly suggest that the physiologically relevant ligands for FF2 are the NPFF-related peptides whereas the NPVF-related peptides are the preferred ligands for FF1.

NPFF-related peptides have been shown to be involved in various somatosensory and visceral functions (8). Perhaps the best characterized action for NPFF is its role in nociception and analgesia (for recent reviews, see Refs. 9 and 39). There is a body of evidence that central administration of NPFF-related peptides produces hyperalgesia and reverses morphine-induced analgesia (5, 9). Intrathecal administration of NPFF, however, produces antinociceptive, pro-opioid effects (14). Since our *in situ* data showed only FF2 expression in rat spinal cord, FF2 most likely mediated the pro-opioid effect of NPFF following intrathecal injection. On the other hand, the anti-opioid effects of intracerebroventricularly administered NPFF were most likely mediated by FF1 based on the following observations. Our data showed that NPSF-(1–37), which had poor if any agonist activity for FF2 but potent activity for FF1, was more potent than NPFF in suppressing morphine-induced analgesia in two models of nociception (Fig. 7). FMRFamide, which displayed no significant agonist activity for FF2 but potent activity for FF1, was equally as potent as NPFF in anti-opioid activity (40). Only FF1 is expressed in the periaqueductal gray (Table II), a region critical for the control of nociception. All together, these *in vitro* and *in vivo* observations strongly suggest that the anti-opioid effects of NPFF were actually mediated by the FF1 receptor, and the real endogenous anti-opioid peptides are NPVF-related peptides. Furthermore, the strong expression of FF1 in the limic system may suggest an important role of NPVF in manifestation of the affective aspects of pain.

REFERENCES

1. Greenberg, M. J., and Price, D. A. (1992) *Prog. Brain Res.* **92,** 25–37
2. Li, C., Kim, K., and Nelson, L. S. (1999) *Brain Res.* **848,** 26–34
3. Weber, E., Evans, C. J., Samuelsson, S. J., and Barchas, J. D. (1981) *Science* **214,** 1248–1251
4. Dockray, G. J., Reeve, J. R., Jr., Shively, J., Gayton, R. J., and Barnard, C. S. (1983) *Nature* **305,** 328–330
5. Yang, H. Y., Fratta, W., Majane, E. A., and Costa, E. (1985) *Proc. Natl. Acad. Sci. U. S. A.* **82,** 7757–7761
6. Perry, S. J., Huang, E. Y.-K., Cronk, D., Bagust, J., Sharma, R., Walker, R. J., Wilson, S., and Burke, J. F. (1997) *FEBS Lett.* **409,** 426–430
7. Vilim, F. S., Aarnisalo, A. A., Nieminen, M. L., Lintunen, M., Karlstedt, K., Kontinen, V. K., Kalso, E., States, B., Panula, P., and Ziff, E. (1999) *Mol. Pharmacol.* **55,** 804–811
8. Panula, P., Aarnisalo, A. A., and Wasowicz, K. (1996) *Prog. Neurobiol.* **48,** 461–487
9. Roumy, M., and Zajac, J. M. (1998) *Eur. J. Pharmacol.* **345,** 1–11
10. Kavaliers, M., and Yang, H. Y. (1989) *Peptides* **10,** 741–745
11. Malin, D. H., Lake, J. R., Hammond, M. V., Fowler, D. E., Rogillio, R. B., Brown, S. L., Sims, J. L., Leecraft, B. M., and Yang, H. Y. (1990) *Peptides* **11,** 969–972
12. Lake, J. R., Hammond, M. V., Shaddox, R. C., Hunsicker, L. M., Yang, H. Y., and Malin, D. H. (1991) *Neurosci. Lett* **132,** 29–32
13. Harrison, L. M., Kastin, A. J., and Zadina, J. E. (1998) *Peptides* **19,** 1603–1630
14. Gouarderes, C., Sutak, M., Zajac, J. M., and Jhamandas, K. (1993) *Eur. J. Pharmacol.* **237,** 73–81
15. Altier, N., Dray, A., Menard, D., and Henry, J. L. (2000) *Eur. J. Pharmacol.* **407,** 245–255
16. Elshourbagy, N. A., Ames, R. S., Fitzgerald, L. R., Foley, J. J., Chambers, J. K., Szekeres, P. G., Evans, N. A., Schmidt, D. B., Buckley, P. T., Dytko, G. M., Murdock, P. R., Milligan, G., Groarke, D. A., Tan, K. B., Shabon, U., Nuthulaganti, P., Wang, D. Y., Wilson, S., Bergsma, D. J., and Sarau, H. M. (2000) *J. Biol. Chem.* **275,** 25965–25971
17. Bonini, J. A., Jones, K. A., Adham, N., Forray, C., Artymyshyn, R., Durkin, M. M., Smith, K. E., Tamm, J. A., Boteju, L. W., Lakhlani, P. P., Raddatz, R., Yao, W. J., Ogozalek, K. L., Boyle, N., Kouranova, E. V., Quan, Y., Vaysse, P. J., Wetzel, J. M., Branchek, T. A., Gerald, C., and Borowsky, B. (2000) *J. Biol. Chem.* **275,** 39324–39331
18. Kotani, M., Mollereau, C., Detheux, M., Le Poul, E., Brezillon, S., Vakili, J., Mazarguil, H., Vassart, G., Zajac, J. M., and Parmentier, M. (2001) *Br. J. Pharmacol.* **133,** 138–144
19. Hinuma, S., Shintani, Y., Fukusumi, S., Iijima, N., Matsumoto, Y., Hosoya, M., Fujii, R., Watanabe, T., Kikuchi, K., Terao, Y., Yano, T., Yamamoto, T., Kawamata, Y., Habata, Y., Asada, M., Kitada, C., Kurokawa, T., Onda, H., Nishimura, O., Tanaka, M., Ibata, Y., and Fujino, M. (2000) *Nat. Cell Biol.* **2,** 703–708
20. Satake, H., Hisada, M., Kawada, T., Minakata, H., Ukena, K., and Tsutsui, K. (2001) *Biochem. J.* **354,** 379–385
21. McDonald, T., Wang, R., Bailey, W., Xie, G., Chen, F., Caskey, C. T., and Liu, Q. (1998) *Biochem. Biophys. Res. Commun.* **247,** 266–270
22. Zlokarnik, G., Negulescu, P. A., Knapp, T. E., Mere, L., Burres, N., Feng, L., Whitney, M., Roemer, K., and Tsien, R. Y. (1998) *Science* **279,** 84–88
23. Conklin, B. R., Farfel, Z., Lustig, K. D., Julius, D., and Bourne, H. R. (1993) *Nature* **363,** 274–276
24. Lynch, K. R., O'Neill, G. P., Liu, Q., Im, D. S., Sawyer, N., Metters, K. M., Coulombe, N., Abramovitz, M., Figueroa, D. J., Zeng, Z., Connolly, B. M., Bai, C., Austin, C. P., Chateauneuf, A., Stocco, R., Greig, G. M., Kargman, S., Hooks, S. B., Hosfield, E., Williams, D. L., Jr., Ford-Hutchinson, A. W., Caskey, C. T., and Evans, J. F. (1999) *Nature* **399,** 789–793
25. Liu, Q., Pong, S. S., Zeng, Z., Zhang, Q., Howard, A. D., Williams, D. L., Jr., Davidoff, M., Wang, R., Austin, C. P., McDonald, T. P., Bai, C., George, S. R., Evans, J. F., and Caskey, C. T. (1999) *Biochem. Biophys. Res.*

Commun. **266,** 174–178
26. Guan, X. M., Yu, H., and Van der Ploeg, L. H. (1998) *Brain Res. Mol. Brain Res.* **59,** 273–279
27. Zimmermann, M. (1983) *Pain* **16,** 109–110
28. Fiering, S., Northrop, J. P., Nolan, G. P., Mattila, P. S., Crabtree, G. R., and Herzenberg, L. A. (1990) *Genes Dev.* **4,** 1823–1834
29. Altschul, S. F., Madden, T. L., Schaffer, A. A., Zhang, J., Zhang, Z., Miller, W., and Lipman, D. J. (1997) *Nucleic Acids Res.* **25,** 3389–3402
30. Andrews, P. C., Brayton, K. A., and Dixon, J. E. (1989) *Experientia Suppl.* **56,** 192–209
31. Seidah, N. G., Day, R., Marcinkiewicz, M., and Chretien, M. (1998) *Ann. N. Y. Acad. Sci.* **839,** 9–24
32. Panula, P., Kivipelto, L., Nieminen, O., Majane, E. A., and Yang, H. Y. (1987) *Med. Biol.* **65,** 127–135
33. Hinuma, S., Habata, Y., Fujii, R., Kawamata, Y., Hosoya, M., Fukusumi, S., Kitada, C., Masuo, Y., Asano, T., Matsumoto, H., Sekiguchi, M., Kurokawa, T., Nishimura, O., Onda, H., and Fujino, M. (1998) *Nature* **393,** 272–276
34. Dupouy, V., and Zajac, J. M. (1996) *Synapse* **24,** 282–296
35. Davis, M. (1998) *Biol. Psychiatry* **44,** 1239–1147
36. Price, D. D. (2000) *Science* **288,** 1769–1772
37. Allard, M., Zajac, J. M., and Simonnet, G. (1992) *Neuroscience* **49,** 101–116
38. Aarnisalo, A. A., and Panula, P. (1995) *Neuroscience* **65,** 175–192
39. Panula, P., Kalso, E., Nieminen, M., Kontinen, V. K., Brandt, A., and Pertovaara, A. (1999) *Brain Res.* **848,** 191–196
40. Tang, J., Yang, H. Y., and Costa, E. (1984) *Proc. Natl. Acad. Sci. U. S. A.* **81,** 5002–5005
41. Zastawny, R. L., and McWhinnie, E. A. (1999) *Canadian Patent Application CA 2,269,192*

MECHANISMS OF SIGNAL TRANSDUCTION:

Identification and Characterization of Novel Mammalian Neuropeptide FF-like Peptides That Attenuate Morphine-induced Antinociception

Qingyun Liu, Xiao-Ming Guan, William J. Martin, Terrence P. McDonald, Michelle K. Clements, Qingping Jiang, Zhizhen Zeng, Marlene Jacobson, David L. Williams, Jr., Hong Yu, Douglas Bomford, David Figueroa, John Mallee, Ruiping Wang, Jilly Evans, Robert Gould and Christopher P. Austin

J. Biol. Chem. 2001, 276:36961-36969.
doi: 10.1074/jbc.M105308200 originally published online July 31, 2001